EUMETSAT

MSG Meteorological Product Operations Validation Report - 1

Release 1.5.1

Doc.No. : EUM/OPS/REP/11/1743
Issue : v1A
Date : 1 June 2011

EUMETSAT
Eumetsat-Allee 1, D-64295 Darmstadt, Germany
Tel: +49 6151 807-7
Fax: +49 6151 807 555
http://www.eumetsat.int

Document Change Record

Issue / Revision	*Date*	*DCN. No*	*Changed Pages / Paragraphs*
v1	25 May 2011		Based on HB #349754 v1C (full document for internal use), edited for Web version as follows: • Shortened signature list. • Sections 3, 4 & 5 combined and simplified.
v1A	1 June 2011		• Editorial changes • Update of Section 2.7 with associated change in Section 3

Table of Contents

1 INTRODUCTION

1.1 Purpose and Scope

Release 1.5.1 is the first official release on a new hardware environment for meteorological product processing. This release not only contains the mandatory changes to the old processing system software as required by the different hardware, operating system and compilers, but also includes several new products and changes to a number of existing products.

The activation of the updated and new products has been spread over a period of nearly two months (see Section 3 for the timeline). In the context of this document references are made to “old” and “new” products, indicating the product “before” and “after” the relevant activation date.

The new and the changed products that are referred to here are:

- Normalised Difference Vegetation Index (new product)
- Aerosol Properties over Sea (new product)
- Volcanic Ash Detection (new product)
- Global Instability Index (existing product with higher resolution)
- Regional Instability Index (existing product with larger coverage area)
- Total Ozone (existing product with higher resolution)
- Active Fire Monitoring (existing product with change in format)

Additional documented changes in the cloud detection lead to slightly different results around the sunglint area around sunset and sunrise. Corrective actions in data supporting the generation of the Active Fire Monitoring product have increased the detection rate of possible and probable fires.

In addition to the product algorithm changes, the following software package updates have been made:

- As radiative transfer model, RTTOV Version 9.3 is used
- The GRIB API is introduced for all GRIB decoding activities (e.g. forecasts)
- The BUFR API is introduced for all decoding and encoding activities

1.2 Document Structure

The document has the following structure.

Section 1: Introduction
This introduction.

Section 2: Product Validation
This section describes a global validation of generated and encoded products.

Section 3: Conclusions

2 PRODUCT VALIDATION

2.1 Sunglint Area Definition Change

Within the cloud detection algorithm, a sunglint area is calculated to avoid using there those channels in the visible region of the spectrum, as the higher reflectances will give rise to misclassifications (too much cloud). Hence, in the sunglint area, only the channels in the infrared spectrum will be used for the determination of the sun type. During twilight conditions the sunglint mask used in the old algorithm is too small, leading to an over-abundant classification of pixels as clouds. The new algorithm makes use of the sea reflectance part of the bi-directional reflectance function (BDRF) model introduced in Section 2.2, enlarging the sunglint mask in the twilight area. It should be noted though that the mask around local noon becomes smaller (see Figure 1).

The change to the algorithm is as follows:

Old mask definition:

$$SunglintAngle < \frac{18}{1 - 0.5 \times [1 - \cos(SolZen)]}$$

$$SunglintAngle = \cos^{-1}[\cos(SolZen)\cos(ViewZen) - \sin(SolZen)\sin(ViewZen)\cos(RelAzi)]$$

New mask definition:

$$SunglintRefl > 0.25$$

$$SunglintRefl = 0.65 \times \frac{1.25 - 0.25\cos(2.SolZen)}{1 + \frac{SunglintAngle}{S_0}}$$

where:

$$S_0 = 0.1 + 0.002 \times SolZen + (k.v_{wind})$$

SolZen = solar zenith angle (in degrees as used in above expression)
ViewZen = viewing zenith angle
RelAzi = relative azimuth angle
k = wind coefficient
v_{wind} = wind speed (in m/s)

Currently, k is set to zero to disable the term $(k.v_{wind})$, but may be used in the future.

Old	New
04:00 UTC	
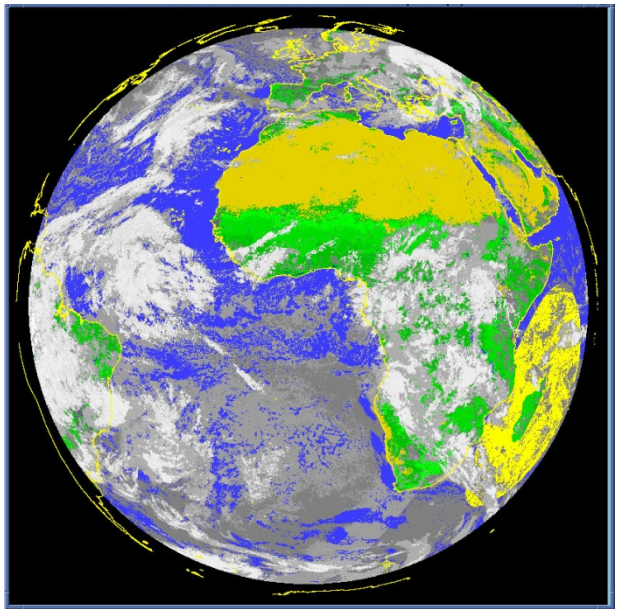	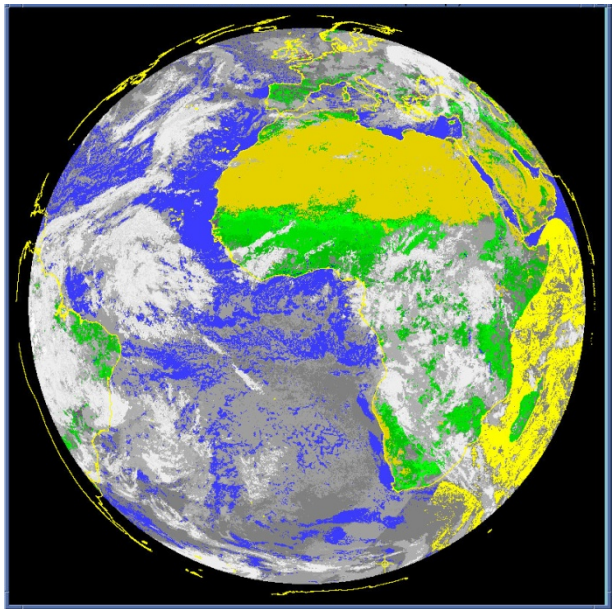
12:00 UTC	
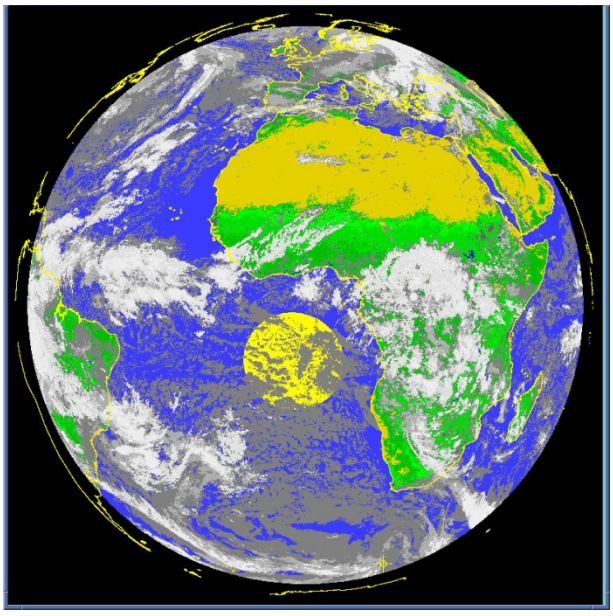	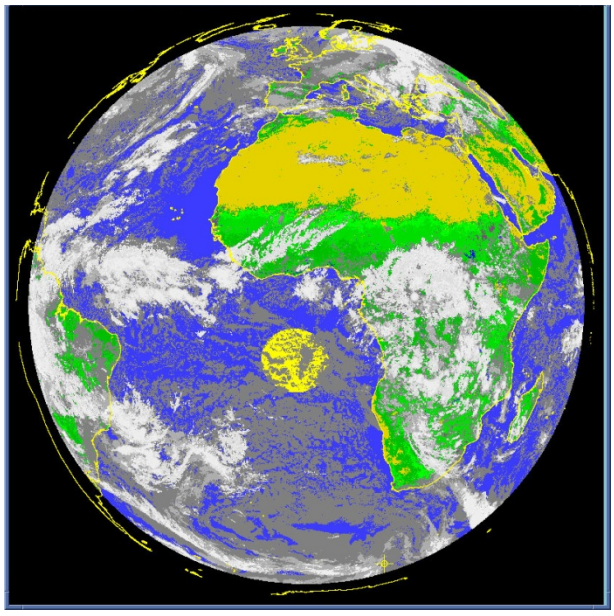

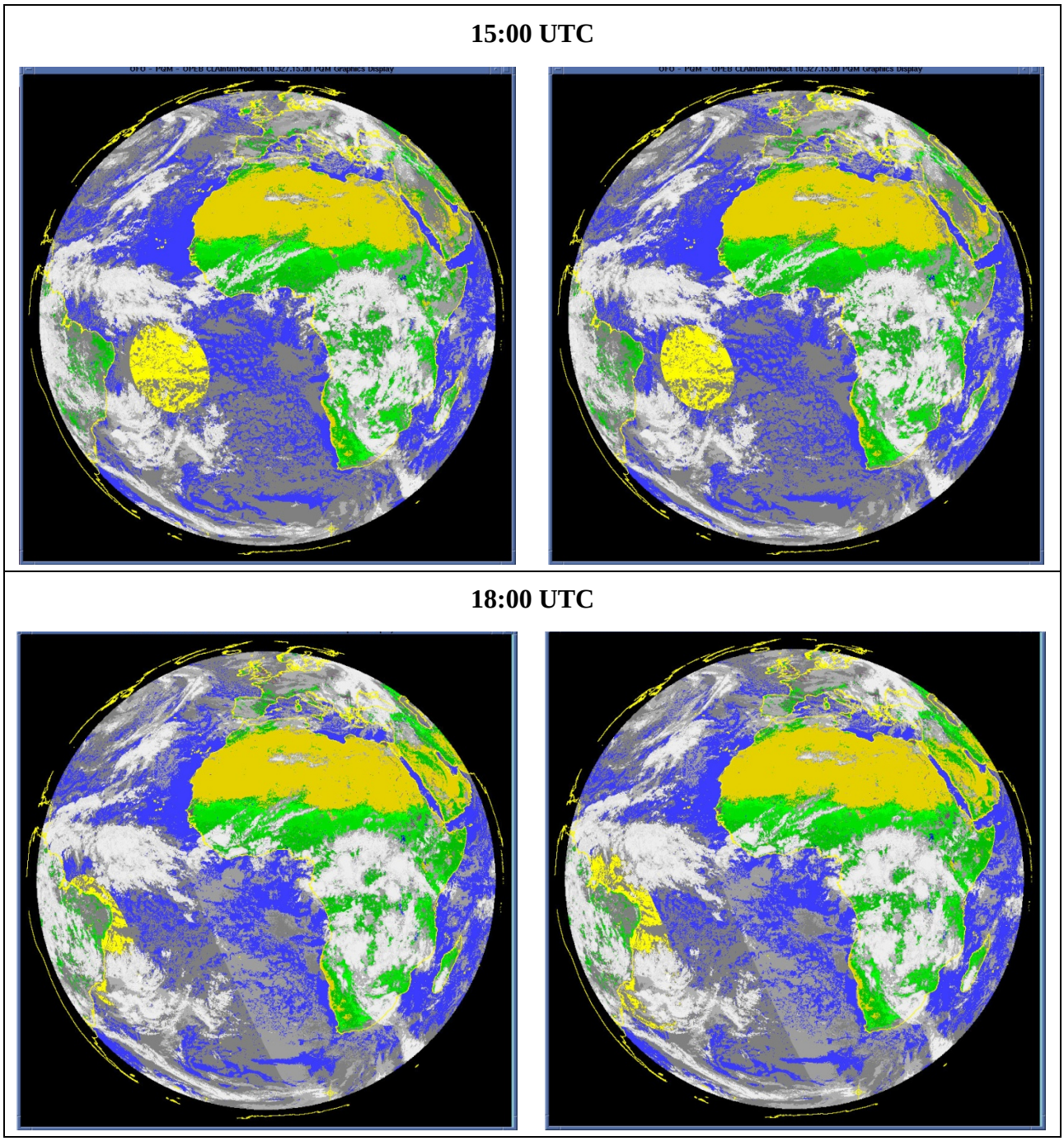

Figure 1: Modified determination of the sunglint mask (indicated by the yellow area) on 23 November 2010 at 04:00, 12:00, 15:00 and 18:00 UTC. The underlying product is the CLA intermediate product Scene type.

The change of the sunglint mask affects the cloud detection within the increased area, especially at sunrise and sunset – see the highlighted examples in Figure 2. However, the changes are not drastic when viewing at larger scales. As an example, it can be seen in Figure 3 that the scenes and cloud type distributions over the African continent are basically unchanged.

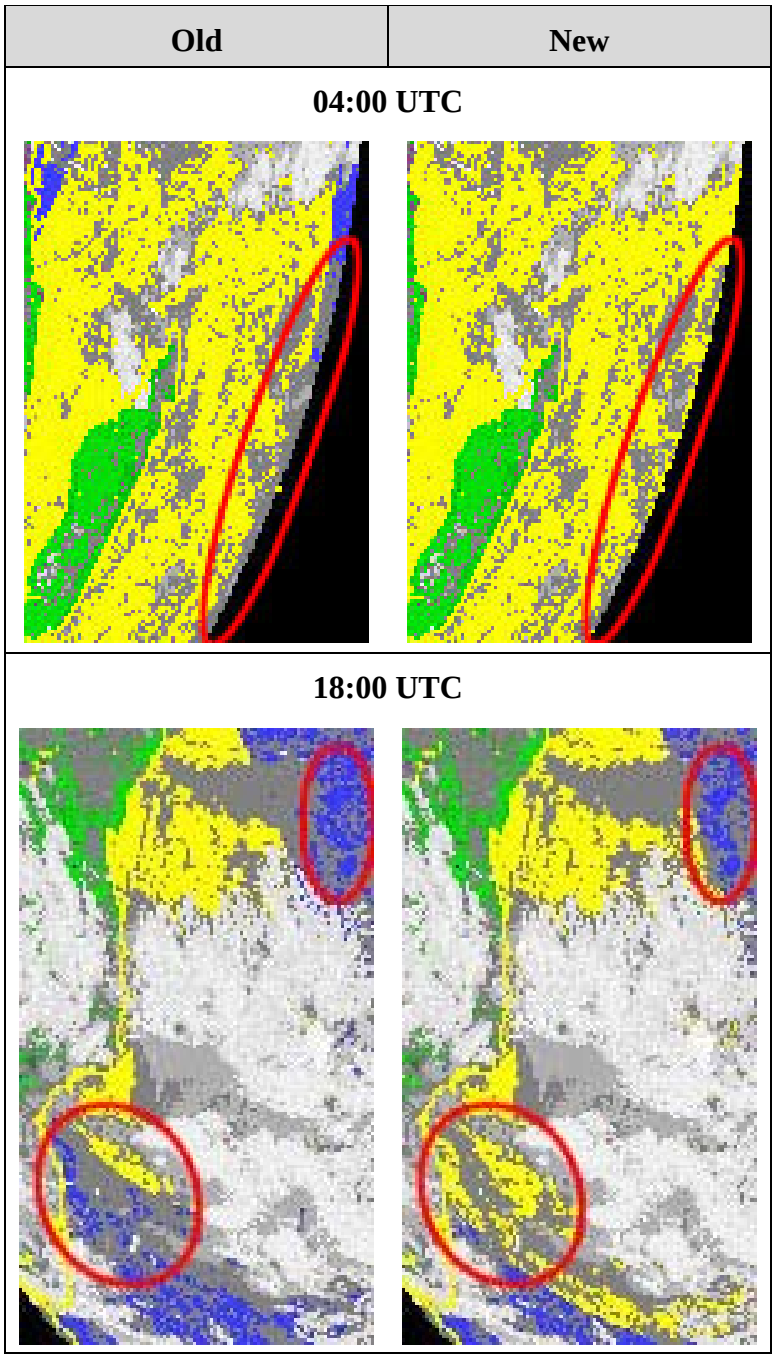

Figure 2: Zoomed-in examples taken from Figure 1, showing cloud detection differences resulting from increased sunglint area

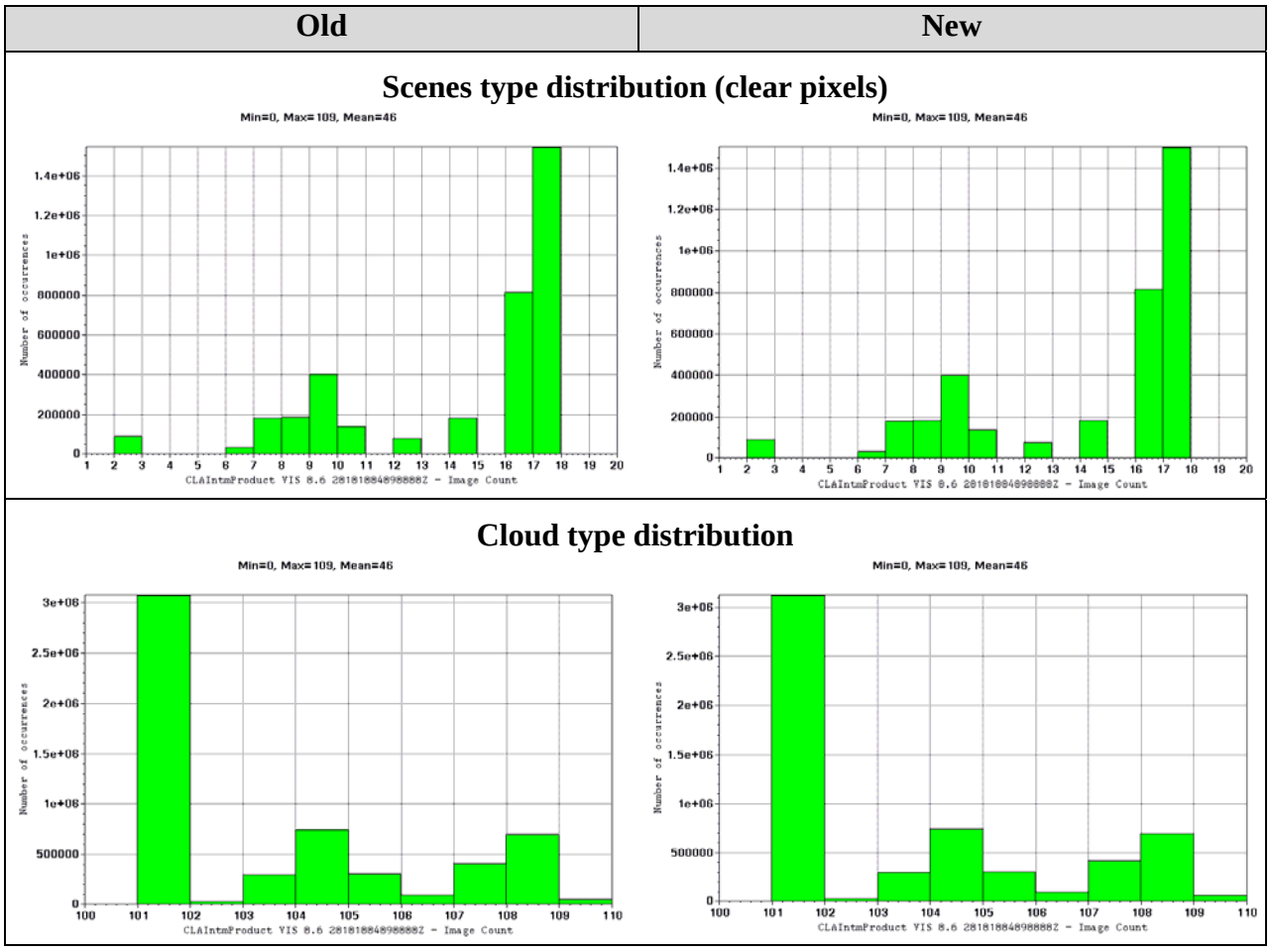

Figure 3: Cumulative distribution histograms for scene types: surface (top figures) and cloud types (bottom figures) on 4 October 2010 9:00 UTC. The left-hand figures show the histograms for the old system, the right-hand figures show them for the new system.

Further information can be found in the following reference documents (available on the EUMETSAT website www.eumetsat.int under the Resources page):

- MSG Meteorological Products Extraction Facility (MPEF) Algorithm Specification Document (EUM/MSG/SPE/022)
- Cloud Detection for MSG - Algorithm Theoretical Basis Document (EUM/MET/REP/07/0132)

2.2 New BDRF Tables

The software for the generation of Meteosat Second Generation (MSG) meteorological products already included the concept of bi-directional reflectance function (BDRF) tables to predict the earth reflectance in the visible channels at various sun and viewing angles. However, this table was up to now set with constant values. The need for a proper BDRF table has been identified at times close to sunset/sunrise to improve the cloud detection under these conditions. Here the two-hourly Clear Sky Reflectance Maps (CRM) do not describe

accurately enough the rapidly changing surface reflectance. The Ross/Roujean semi-empirical kernel model (Roujean *et al.*,1992 (full reference below), also used by the LAND-SAF for BDRF and albedo determination) has been selected, with the advantage of being linear, and hence easy to invert against observations. The model has three terms representing respectively the isotropic, geometric (shading effects) and volumic (multiple reflections) contributions. A fourth specular reflection term has been added for the reflectance over water and deserts.

Further information can be found in the following reference documents (available on the EUMETSAT website under the Resources page) and literature:

- MSG MPEF Algorithm Specification Document (EUM/MSG/SPE/022)
- Cloud Detection for MSG - Algorithm Theoretical Basis Document (EUM/MET/REP/07/0132)
- Roujean *et al.*,1992: A bi-directional reflectance model of the earth's surface for the correction of remote sensing data, *Journal of Geophysical Research*, vol. 97, pp. 20,455 – 20,468

2.3 Global Instability Index (GII) Product

The Global Instability Index product has not changed with respect to the algorithm. However, it has changed in resolution. Instead of GII observations on a 15x15 pixel grid, now a 3x3 pixel grid is used. As an illustration of the resolution difference, the Total Precipitable Water for the 13:45 UTC GII product from 22 September 2010 is presented in Figure 4 (and see also Figure 7).

Figure 5 compares count distribution histograms of three GII indices – K Index (KI), Lifted Index (LI) and Total Precipitable Water Content (TPW) – for the old and new products for 12 October 2010 07:45 UTC. As expected, the histograms from the new product show considerably higher counts because of their reduced segment size of 3x3 pixels (in comparison to the old product with 15x15 pixels). However, all of the parameters show an almost identical shape in the histograms for each index, providing verification of the successful implementation of the GII product on the new system.

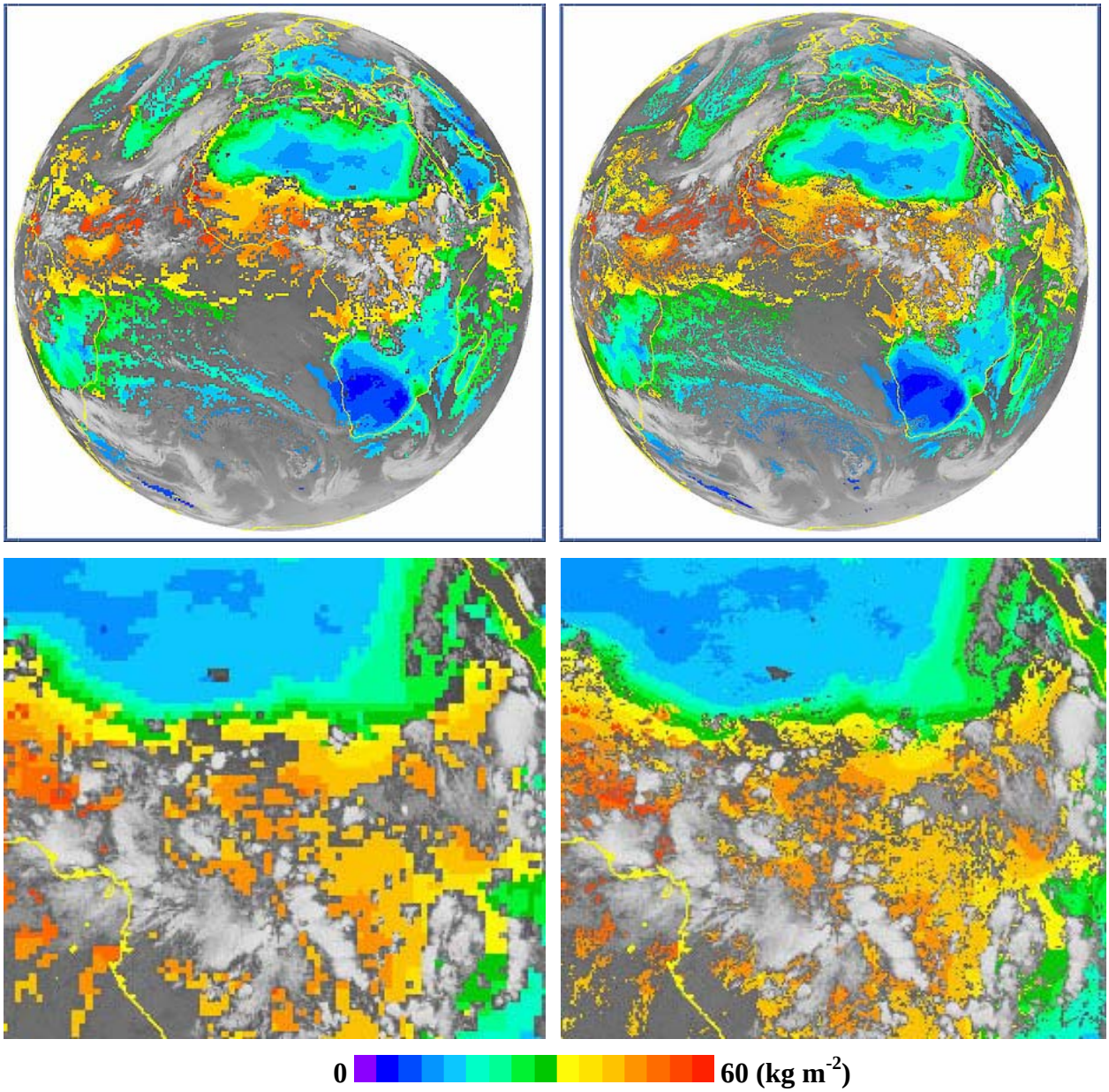

Figure 4: Total Precipitable Water Content in the GII product on 22 September 2010 at 13:45 UTC, showing full disc (top) and a zoomed-in area over central Africa (lower). The left-hand figures show the old product on a 15x15 pixel grid, the right-hand figures show the new product on a 3x3 pixel grid.

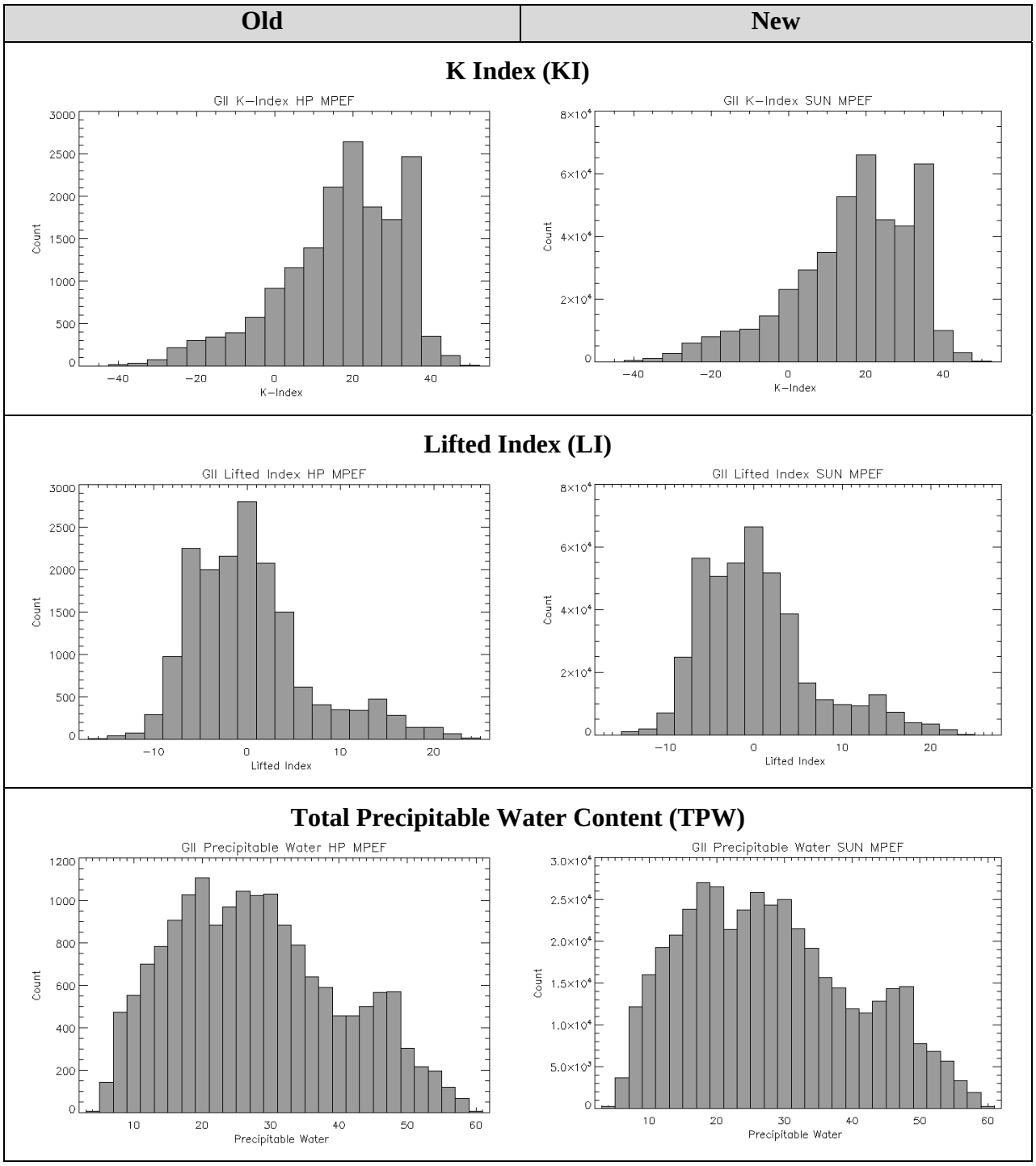

Figure 5: Cumulative distribution histograms for GII K Index (KI), Lifted Index (LI) and Total Precipitable Water Content (TPW) on 12 October 2010 07:45 UTC. The left-hand figures show the histograms for the old system, the right-hand figures show them for the new system.

Further information can be found in the following reference documents (available on the EUMETSAT website under the Resources page):

- MSG MPEF Algorithm Specification Document (EUM/MSG/SPE/022)
- The Global Instability Indices Product Algorithm Theoretical Basis Document (EUM/MET/REP/07/0164)

2.4 Regional Instability Index (RII) Product

The Regional Instability Index product has not changed with respect to the algorithm. It is still a pixel-based product. However, there was a major change to the processing area. Instead of generating the product over part of central Europe only, the new product covers all of Europe up to 60°N. As an illustration of the area covered, the K-Index for 2 December 2010 11:00 UTC is presented in Figure 6.

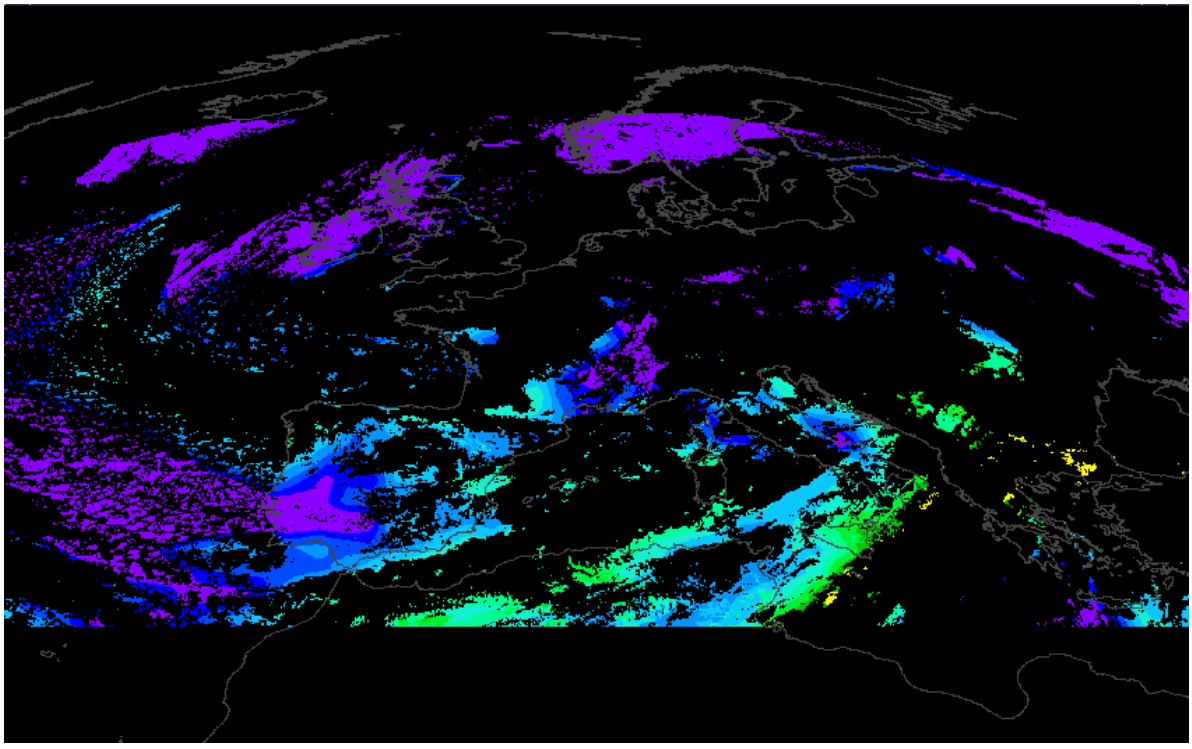

Figure 6: A representation of the area covered by the RII product (K-Index) for 2 December 2010 11:00 UTC

Figure 7 demonstrates the difference between the RII and the old and new GII products by looking at a specific area, for which Western Europe and the adjoining Atlantic was chosen. It is clear that the RII product has a better resolution, but at the cost of containing somewhat more noise. These two products have been disseminated as demonstrational GIIHD and RIIHD products via the EUMETCast trial service to the National Meteorological Services and manufacturers.

For operations it should be noted that the RII product shall be generated only within the Meteosat-8 Rapid Scanning Service, while the global 3x3 GII product shall be generated only within the Meteosat-9 0° service.

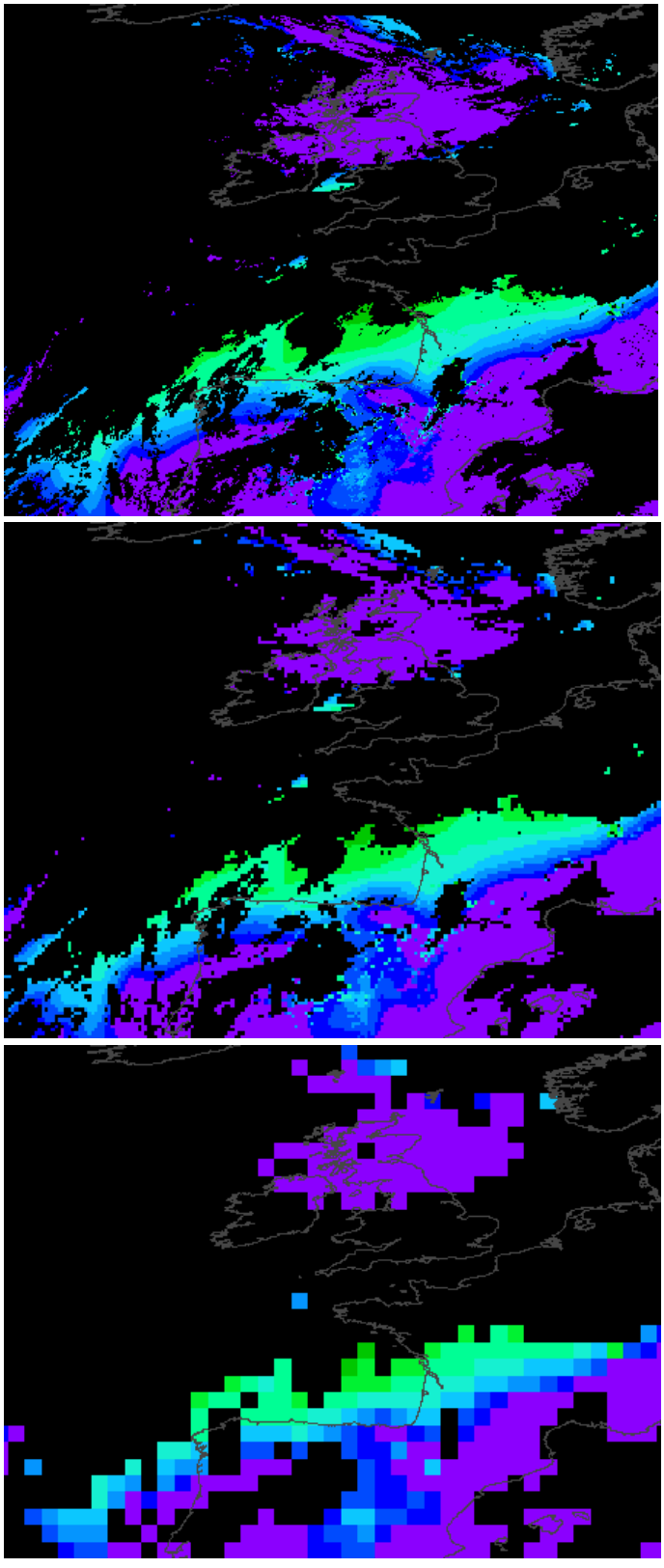

The K-Index of the pixel-based RII product for 10 February 2011 at 13:00 UTC. The figure shows a zoomed area of W. Europe and the adjoining Atlantic only.

As the top figure, but now the K-Index of the 3x3 pixel GII product...

...and now the 15x15 pixel GII product.

Figure 7: A comparison between a selected area from the RII product (K-Index) for 10 February 2011 13:00 UTC (top figure) and the same parameter from the GII 3x3 pixel product (middle figure) and GII 15x15 pixel product (bottom figure)

Further information can be found in the following reference documents (available on the EUMETSAT website under the Resources page):

- MSG MPEF Algorithm Specification Document (EUM/MSG/SPE/022)
- The Global Instability Indices Product Algorithm Theoretical Basis Document (EUM/MET/REP/07/0164)

2.5 Aerosol Properties over Sea (AES) Product

The Aerosol Properties over Sea product is a new product that is derived using a pre-calculated look-up table, and uses the information from the VIS0.6, VIS0.8 and NIR1.6 µm channels from the SEVIRI instrument on Meteosat-9. The output of the product is the aerosol optical depth in these channels together with a quality flag.

An intermediate product is derived for every image containing information in the visible channels, and accumulated around midnight to form a final daily product. This final product is archived and disseminated to the user community. It should be noted that the final product is an average of 3x3 pixels, while the intermediate products are on pixel level. A sample final product is displayed in Figure 8, where we can distinguish dust plumes west of Africa, characterised by higher optical thickness and lower Angstrom coefficient values. The image centre is always relatively noisy because of the sunglint effect.

AOT channel 1 (VIS0.6)

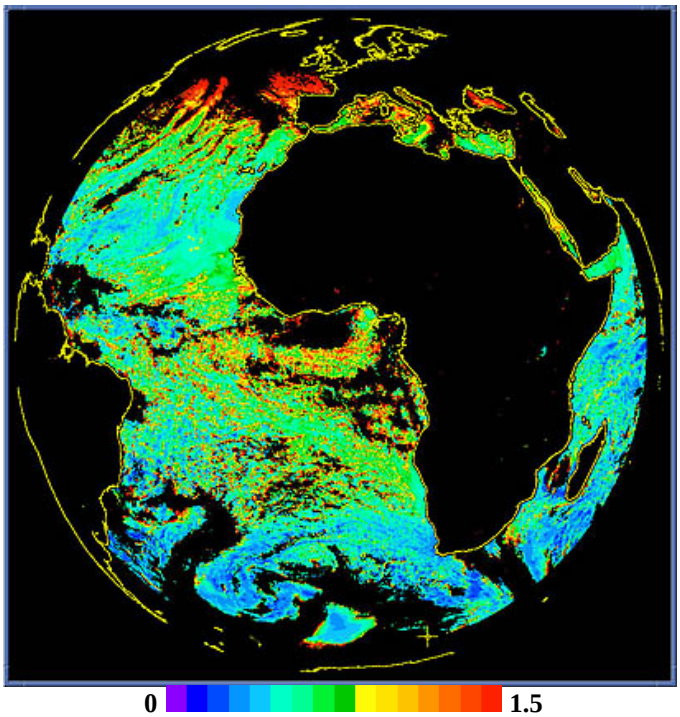

AOT channel 2 (VIS0.8)

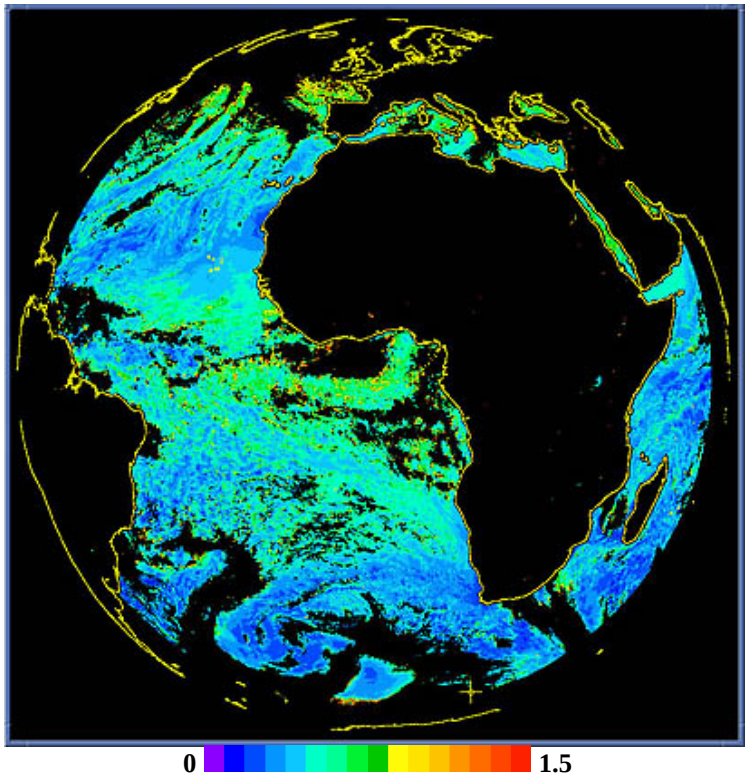

AOT channel 3 (NIR1.6)

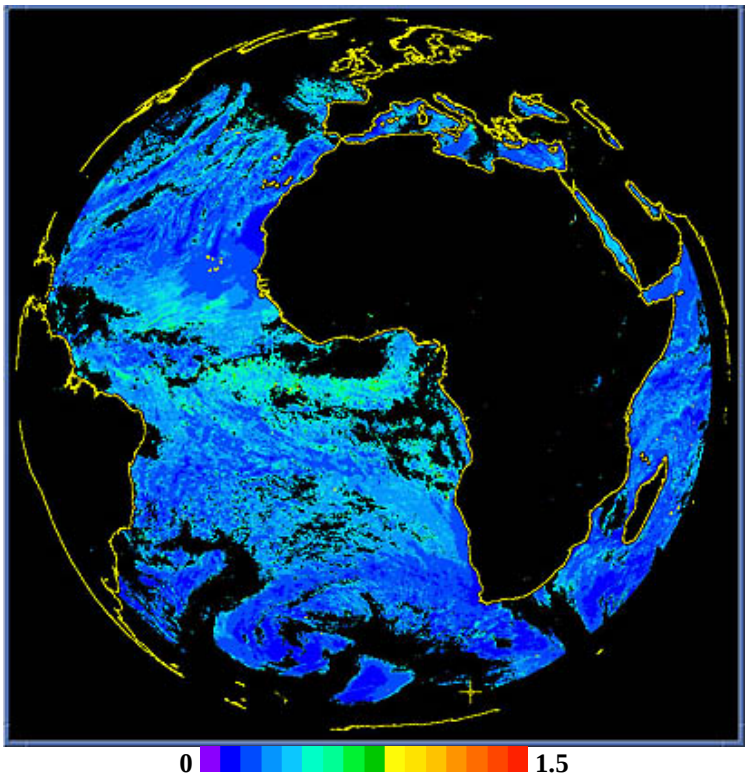

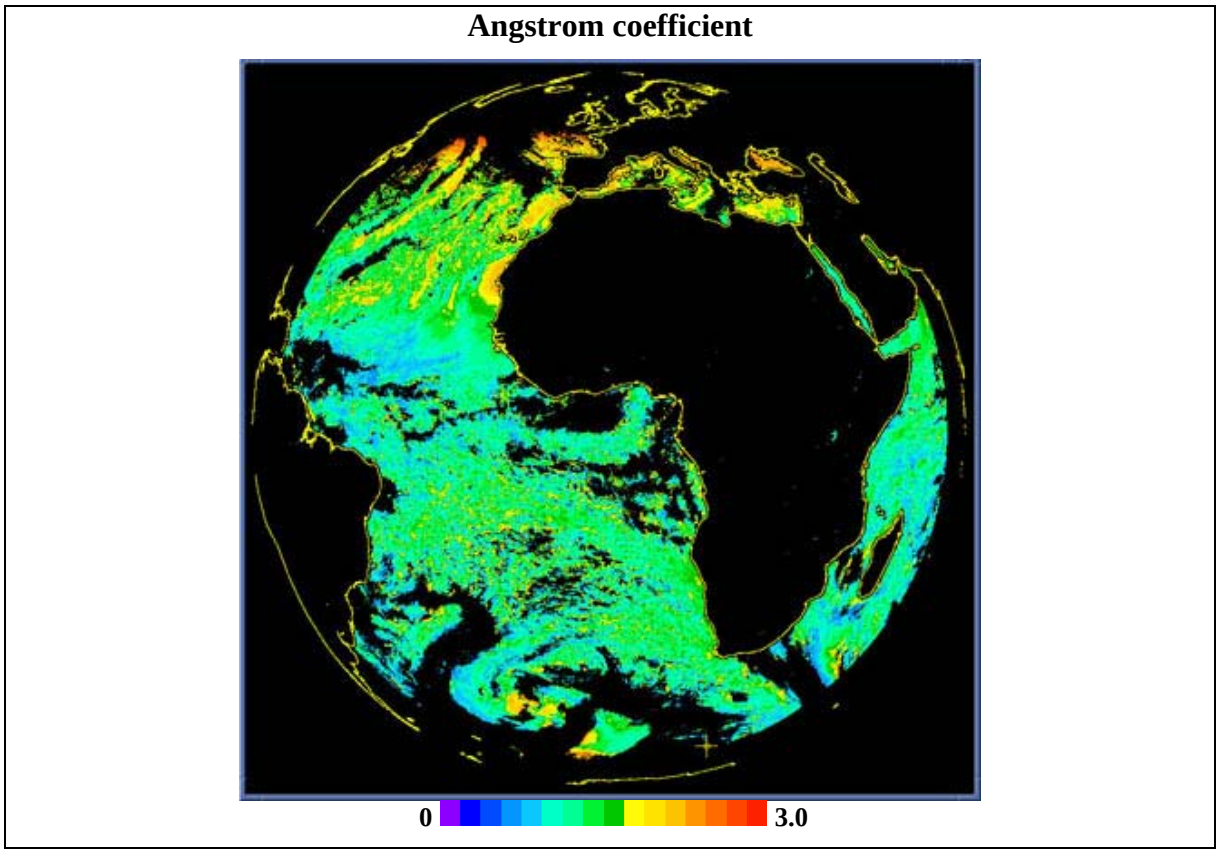

Figure 8: Aerosol Optical Thickness (AOT) for the three visible channels and Angstrom coefficient from the Aerosol final product on 23 November 2010

Further information can be found in the following reference document describing the algorithm (available on the EUMETSAT website under the Resources page) and literature describing the theoretical background (Ignatov and Stowe):

- MSG MPEF Algorithm Specification Document (EUM/MSG/SPE/022)
- Ignatov and Stowe, 2002: Aerosol retrievals from individual AVHRR channels, Part I: Retrieval algorithm, and transition from Dave to 6S RTM", *J. Atmos. Sci.*, 59, 313-334

2.6 Normalised Difference Vegetation Index (NDVI)

As part of the Scenes algorithm, a daily NDVI product is now generated. NDVI products derived from AVHRR/NOAA data are being used widely, typically in user communities dealing with e.g. agriculture and forestry. AVHRR NDVI products suffer, especially in the tropical regions, from the infrequent observations from the AVHRR system. It is thought that the MSG type of spacecraft may add a valuable contribution to the AVHRR data set, improving the cover in time and space.

The algorithm is based on a normalisation of the differences of the NIR 0.81 µm and VIS 0.64 µm channels of the MSG spacecraft.

$$NDVI = (R_{nir} - R_{vis}) \ / \ (R_{nir} + R_{vis})$$

where:

R_{nir} = Near-infrared reflectance (0.81 µm)
R_{vis} = Visible reflectance (0.64 µm)

A cloud detection algorithm processes individually each MSG image that contains useful information within the visible channels – hence, typically between local sunrise and sunset. Within the cloud detection algorithm the NDVI is determined for every pixel for which the following criteria apply:

- The pixel contains valid information from the visible channel.
- The solar zenith angle is less than 76°.
- The probability of the presence of cloud in the pixel is less than 40%.
- The cloud detection uses a sunglint flag over water bodies only. Hence, the number of pixels over land used for the NDVI determination is not affected by the sunglint mask.
- No NDVI value is determined over water bodies. Hence, there is a dependency between the use of a high-resolution land-sea mask and the rectification accuracy: some clear sky pixels might be classified as water surface, while in fact being a land surface pixel (or vice versa).

For subsequent images the NDVI determination is repeated and the following parameters are determined for every pixel as a final product for the day in question: the maximum NDVI value, the minimum NDVI value, the averaged NDVI value together with the number of accumulations during the course of a day.

Two examples are given in Figure 9 for different dates, 21 September and 23 November 2010 (top and bottom images respectively). One can note the difference in the vegetation pattern, corresponding to the decay of the vegetation in the North (autumn for Europe, end of the wet season over Sahel) and vegetation starting to develop in the South.

Further information can be found in the following reference document (available on the EUMETSAT website under the Resources page):

- MSG MPEF Algorithm Specification Document (EUM/MSG/SPE/022)

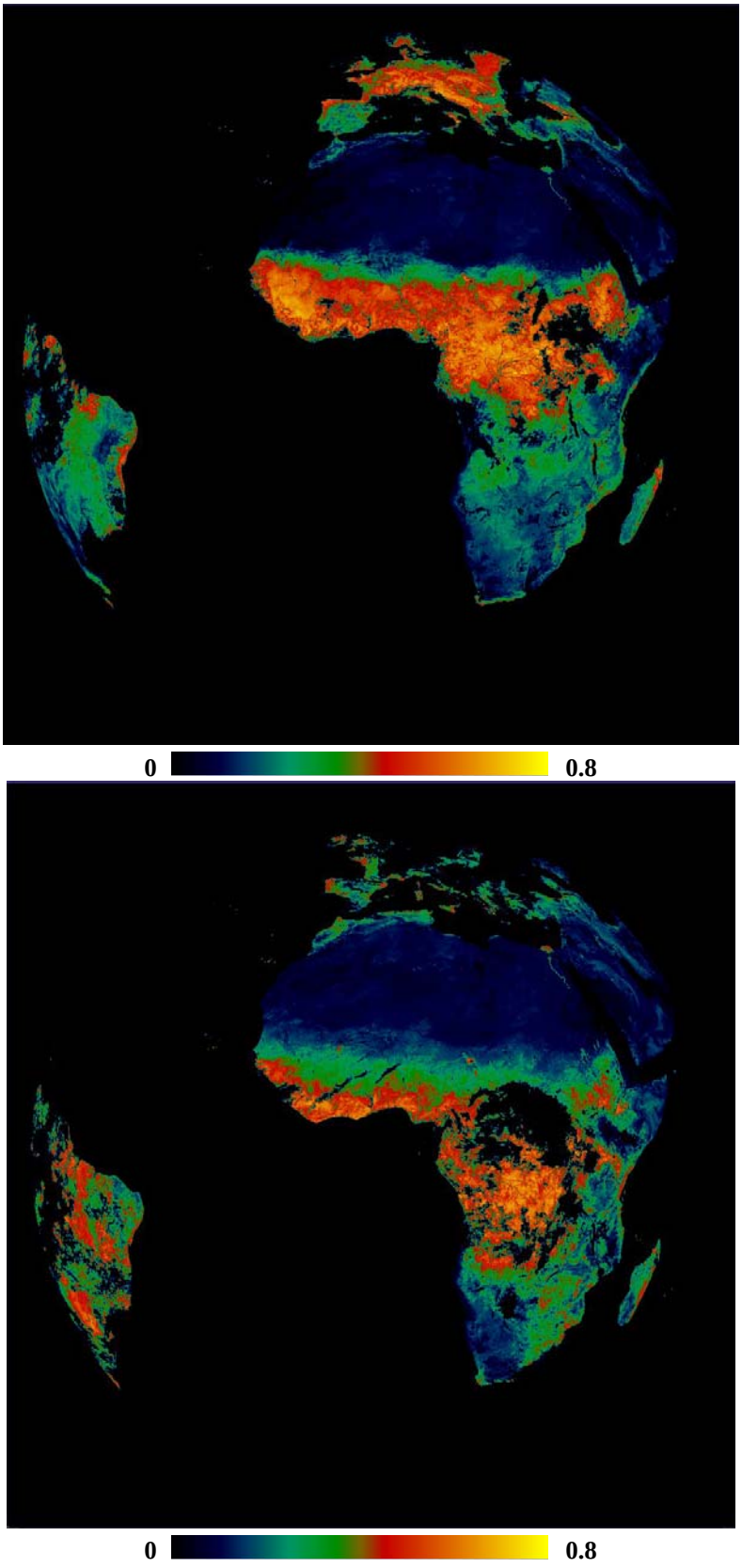

Figure 9: NDVI product generated on 21 September 2010 (top) and 23 November 2010 (bottom). Red areas correspond to dense vegetation, blue to deserts.

2.7 Active Fire Monitoring (FIR) Product

The initial verification of the FIR product revealed differences. However, they seem to be in the right direction: the initial visual inspection suggested that the new product was better than the current old product. In Figure 11 it is clear that, in Eastern Africa especially, the number of detected fires has increased. This was confirmed by Figure 10 which shows statistics of possible and probable fire numbers over about 2½ days (30 January to 1 February 2011), for both the old and new FIR products. Figure 10, which depicts results for the full Earth disc, shows that the new product is detecting more fires, both possible and probable.

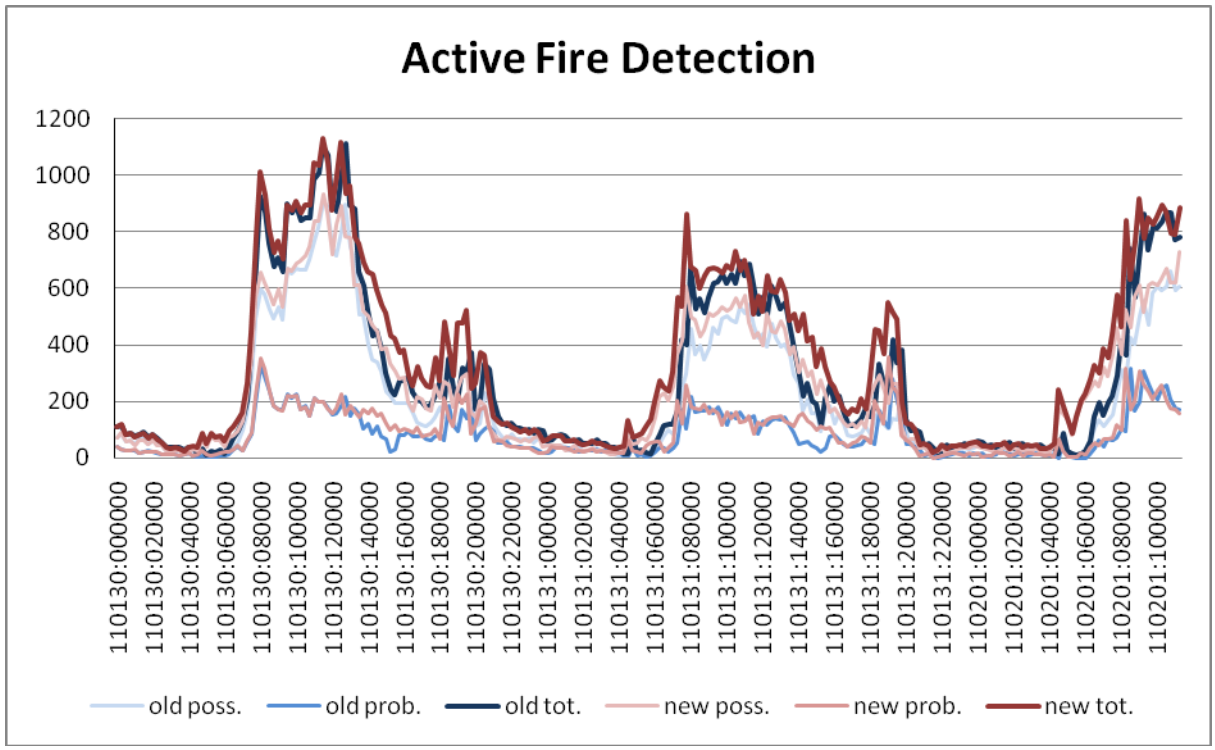

Figure 10: Comparison plots of old and new global FIR results for 30 January to 1 February 2011, showing possible/probable numbers of fires

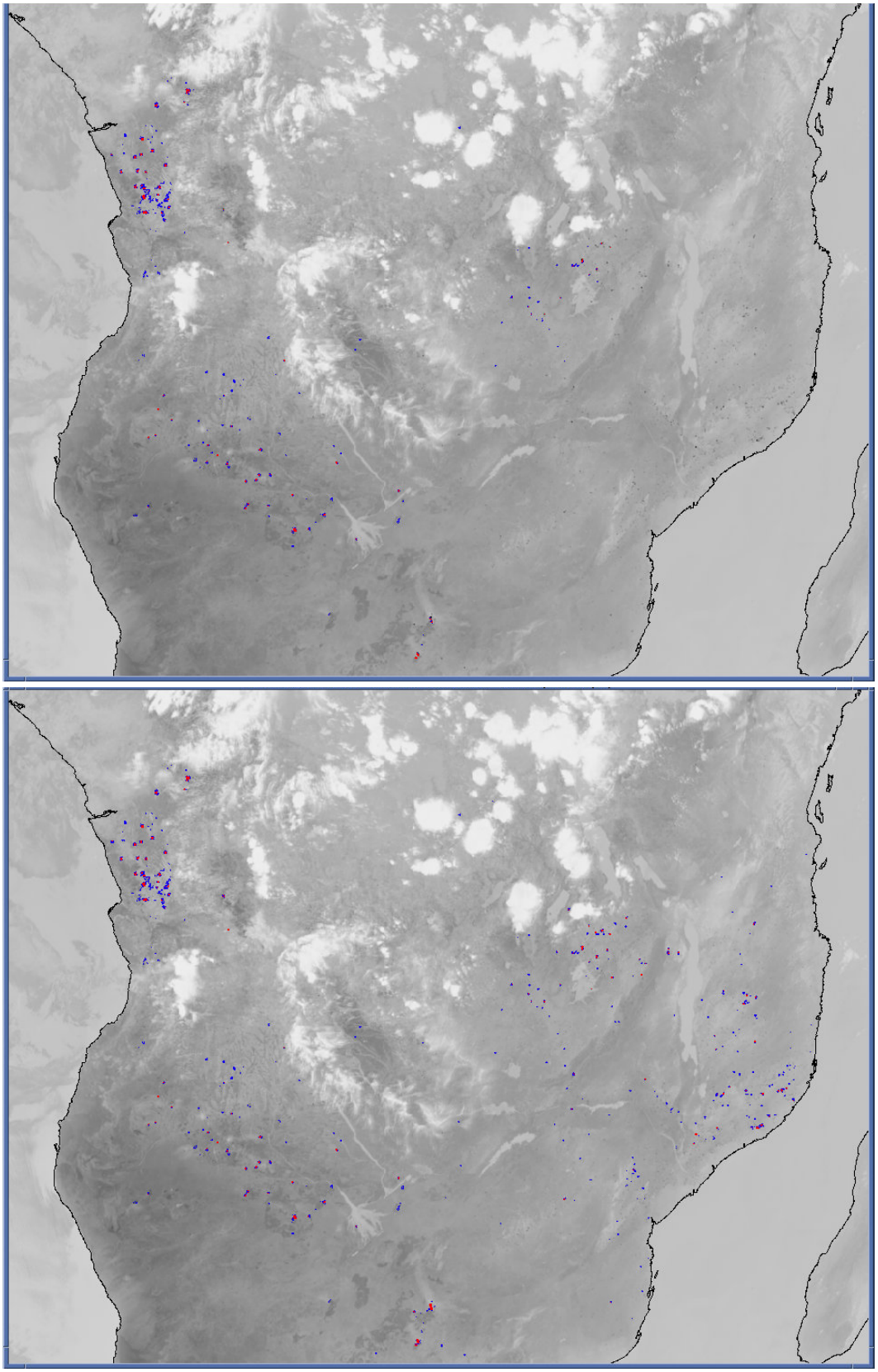

Figure 11: The FIR products from 22 September 2010 14:00 UTC. The top figure shows the old product, while the bottom figure shows the product derived on the new system. The background displays the image from the IR3.9 µm channel.

However, shortly after the new system was rolled out into operations, a larger number of false alarms over Europe were detected. These false alarms were caused by a combination of two effects. During late winter the brightness temperatures for the 10.8 µm channel were low, due to cold surfaces (e.g. snow-covered land, clouds) and the used forecast temperatures were also low. The latter have an influence on the determination of the thresholds for which fire is detected. The major reason for the false alarms is the fact that in this period the solar radiation is increasing, which has an impact on the daytime temperatures in the 3.9 µm channel. For water clouds in particular, warm 3.9 µm channel brightness temperatures with a large contrast between the water clouds and the colder surfaces were detected. This also explains why these false alarms were only detected during daytime. This was confirmed by a slowly decreasing false alarm rate once the surface temperatures and forecasts became warmer.

Nevertheless, a solution reducing the impact of the above feature was identified and introduced for validation for a further update of the product. One of the tests for the fire product states that the reflectance in the VIS 0.6 µm channel shall be less than 30%. This value was reduced to 20%, and the results described below use this update as baseline. The monitoring statistics for Meteosat-9 possible and probable fires (see Figure 12) indicate a lower detection rate for both types. Hence, there is an impact using the new threshold for the VIS channel.

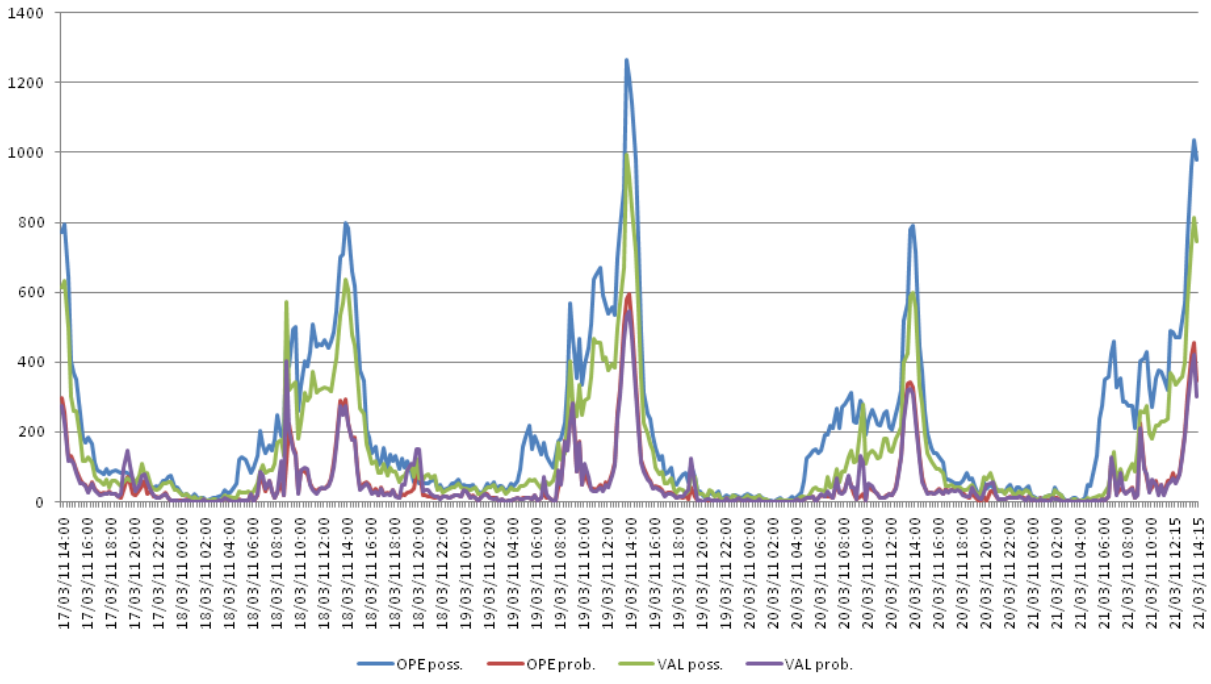

Figure 12: This graph displays the monitoring of the probable and possible fire detections on the new system (indicated as OPE curves) after its operational introduction on 17 February 2011. In addition, the statistics for the product using the new VIS threshold are presented as VAL curves.

An example for the false alarms in Europe is presented in Figure 13. These false alarms have been completely removed by the updated test for the VIS channel. A larger number of

individual cases over Europe have been verified, and in all cases the false alarms have been removed. Nevertheless, the investigation on these false alarms is ongoing. Furthermore, Figure 14 shows the impact of the change of the VIS threshold over East Africa.

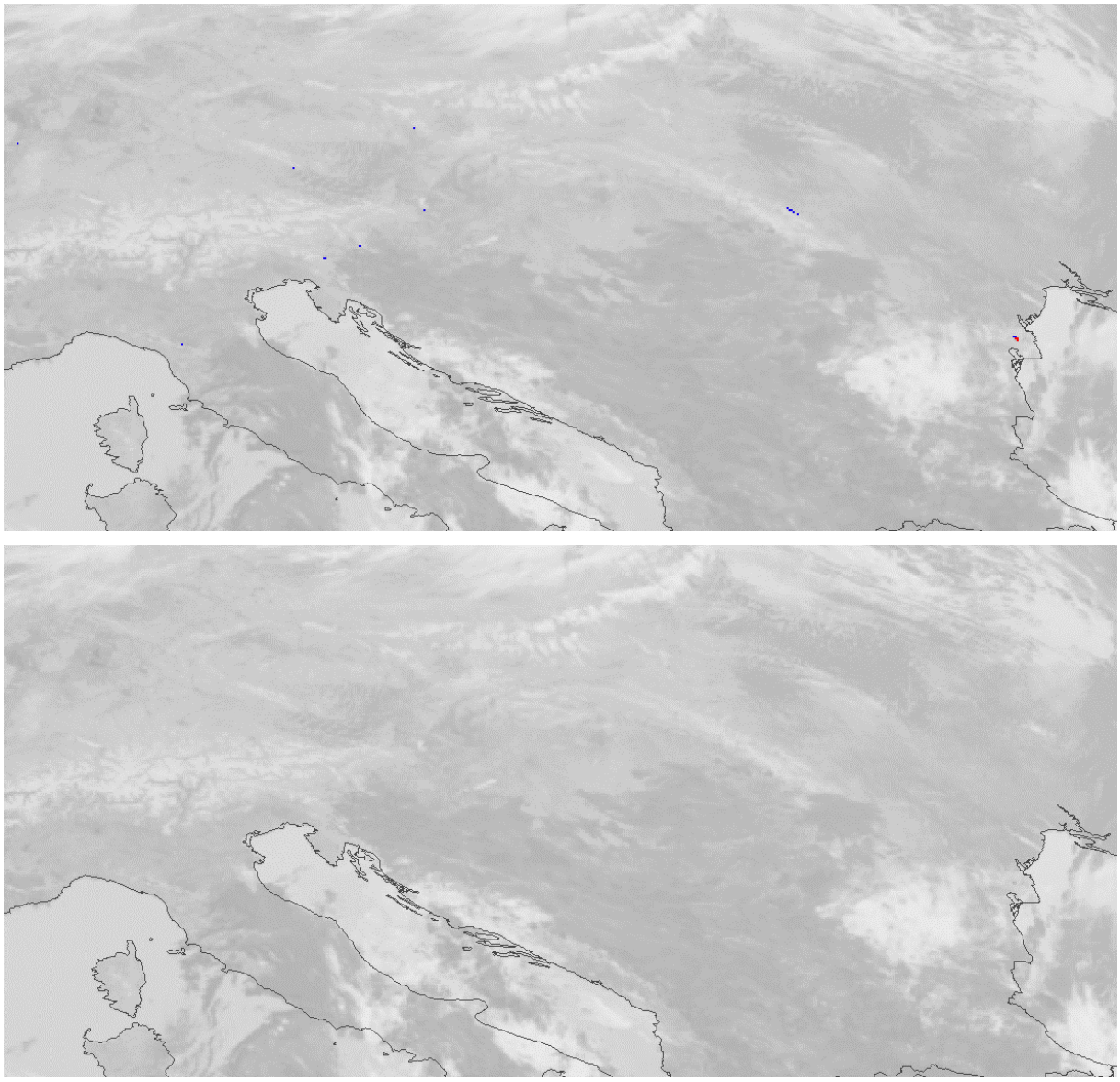

Figure 13: The top figure displays an example of the probable and possible fire detections on the new system after its operational introduction on 17 February 2011. The product is from 21 March 2011 11:45 UTC, for part of the European region. In addition, the same result for the product using the new VIS threshold is presented in the bottom figure.

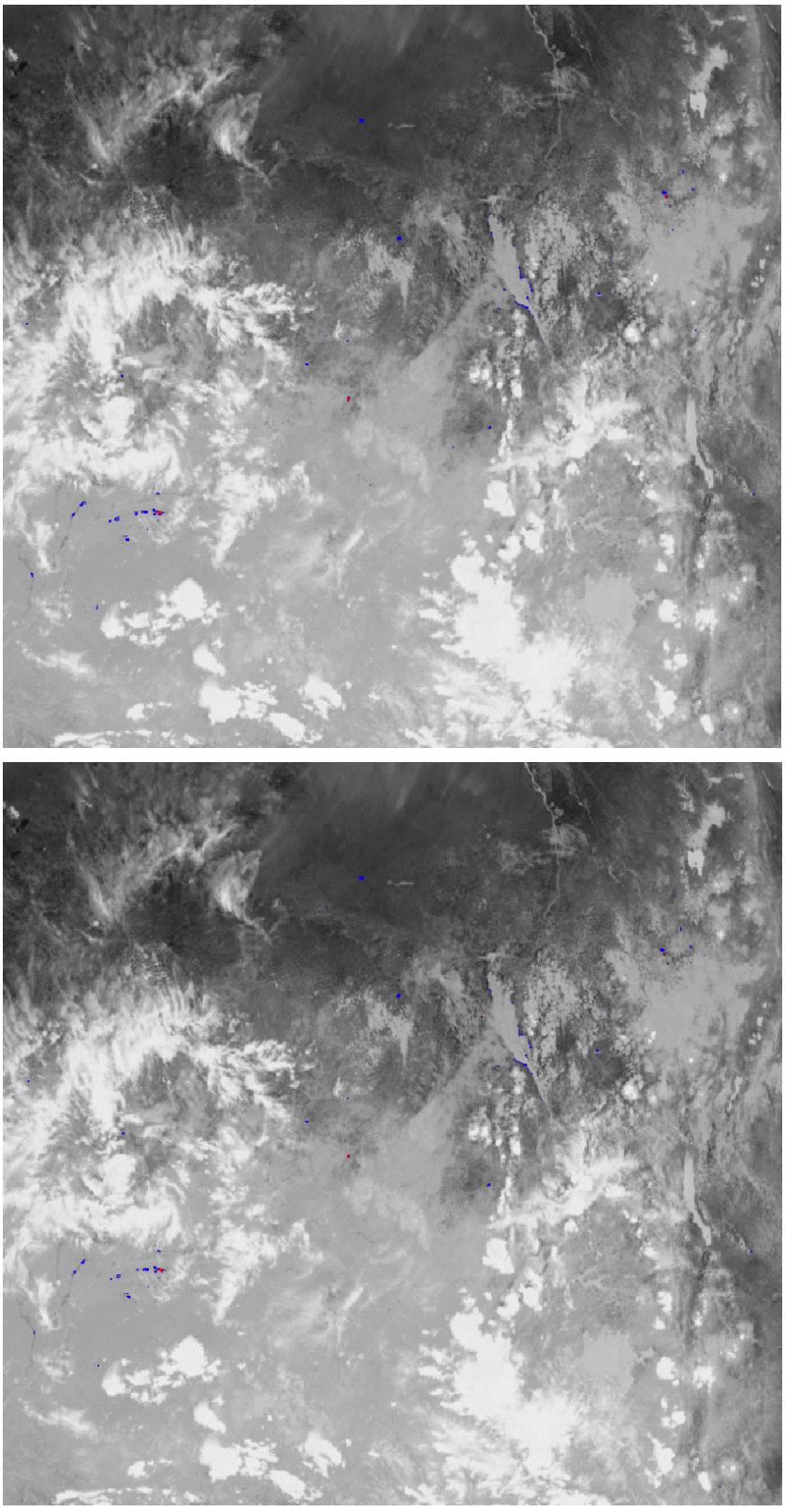

Figure 14: The top figure displays an example of the probable and possible fire detections on the new system after its operational introduction on 17 February 2011. The product is from 21 March 2011 11:45 UTC and shows Eastern Africa. In addition, the same result for the product using the new VIS threshold is presented in the bottom figure.

Further information can be found in the following reference documents (available on the EUMETSAT website under the Resources page):

- MSG MPEF Algorithm Specification Document (EUM/MSG/SPE/022)
- Active Fire Monitoring with MSG Algorithm Theoretical Basis Document (EUM/MET/REP/07/0170)

2.8 Total Ozone (TOZ) Product

The TOZ product generation frequency and its resolution have changed. The old product is an average of four intermediate products and has a 16x16 pixel resolution. The new product has a 3x3 pixel resolution and is generated from a single repeat cycle. It should be noted that the science behind the TOZ algorithm has not changed. The TOZ product shall be disseminated for every repeat cycle.

Figure 15 shows the TOZ products in both resolutions for 18 November 2010 09:45 UTC. Note that the product from the new system is derived from a single repeat cycle.

Further information can be found in the following reference document (available on the EUMETSAT website under the Resources page):

- MSG MPEF Algorithm Specification Document (EUM/MSG/SPE/022)

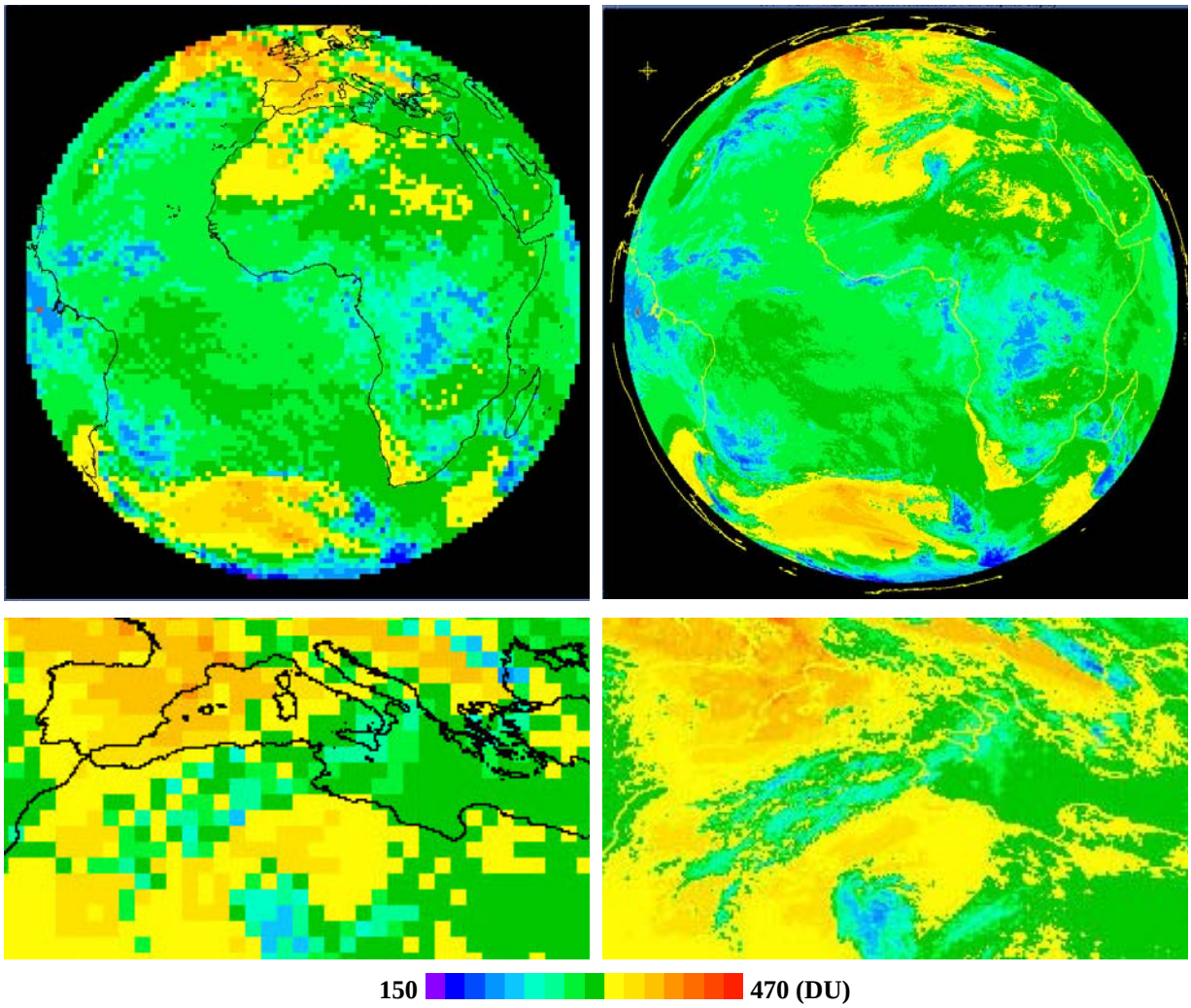

Figure 15: The TOZ products from 18 November 2010 09:45 UTC, with the lower figures showing a zoomed-in area. The left-hand figures show the old TOZ product, while the right-hand figures show the product derived on the new system with an improved resolution.

3 CONCLUSIONS

3.1 Product Validation Summary

The facility generating meteorological products from Meteosat-8 and Meteosat-9 has been modified in two aspects. Besides the change of the hardware platform, the following changes in the meteorological products have been released:

- The Meteosat-9 Total Ozone product is generated for every repeat cycle and has a resolution of 3x3 pixels (formerly 16x16 pixels).
- The Meteosat-9 Global Instability Index has a resolution of 3x3 pixels (formerly 15x15 pixels).
- The format of the Active Fire Monitoring product has been replaced by a CAP format (an xml-based text message).
- The new daily Aerosol Properties over Sea product has been declared a **demonstration** product. The product is generated and archived (note that this product is not disseminated via EUMETCast but is available from the EUMETSAT Data Centre).
- The new daily NDVI product has been declared a **pre-operational** product for dissemination via EUMETCast.
- The new Volcanic Ash Detection product has been introduced as a **demonstration** product.
- For information concerning the Meteosat-8 Global Instability Index product and the Regional Instability Index product, the reader is referred to Section 3.2.

3.2 Timeline of Product Rollout

The timeline for the rollout was as follows for the 0 degree service (= 0°) and the Rapid Scanning Service (= RSS):

17 February 2011

- NDVI (new product) – daily to EUMETCast and daily to EUMETSAT Data Centre.
- AER (new product) – daily to Data Centre.
- GII (0°) – every 15 minutes to EUMETCast and Data Centre, which implies no change. Only the product resolution has increased, indicating a larger product.
- RII (0°) – every 15 minutes to EUMETCast and Data Centre, which implies no change. Only the area coverage increased, indicating a larger product.
- VOL (new product) – which will not be activated yet (CAP and PNG formats).

24 February 2011

- RII (RSS) – every 15 minutes to EUMETCast and Data Centre, which implies no change. Only the area coverage increased, indicating a larger product.

24 March 2011

- Total Ozone (0°) – hourly to EUMETCast, 3-hourly to GTS, every 15 minutes to Data Centre. The resolution and the product generation frequency have changed.
- FIR (0° & RSS) – update of the VIS threshold test to reduce the impact of the false

alarms over Europe.
- FIR (0° & RSS) – format change from local ASCII format to CAP format.
- RII (RSS) – every 5 minutes to EUMETCast and Data Centre.
- Discontinue RII (0°).
- Discontinue GII (RSS).

3.3 Product Status

The following table reflects the status of the MSG meteorological products as per 24 March 2011.

Product	Acronym	Status	Product	Acronym	Status
Active Fire Monitoring	FIR	Demonstration	Cloud Top Height	CTH	Operational
Aerosol Properties over Sea	AES	Demonstration	Divergence	DIV	Operational
All Sky Radiances	ASR	Operational	Global Instability Index	GII	Operational
Atmospheric Motion Vectors	AMV	Operational	Multi-Sensor Precipitation Estimate	MPE	Operational
Clear Sky Reflectance Map	CRM	Operational	Normalised Difference Vegetation Index	NDVI	Pre-Operational
Clear Sky Radiances	CSR	Operational	Regional Instability Index	RII	Operational
Climate Data Set	CDS	Operational	Total Ozone	TOZ	Operational
Cloud Analysis	CLA	Operational	Tropospheric Humidity	TH	Operational
Cloud Analysis Image	CLAI	Operational	Volcanic Ash Detection	VOL	Demonstration
Cloud Mask	CLM	Operational			

Table 1: The status of the MSG meteorological products at 24 March 2011 is indicated. This status is valid, unless specifically stated otherwise, for both 0° and RSS services and for the various formats of the products.